He et. al. Supplementary Figure 1.

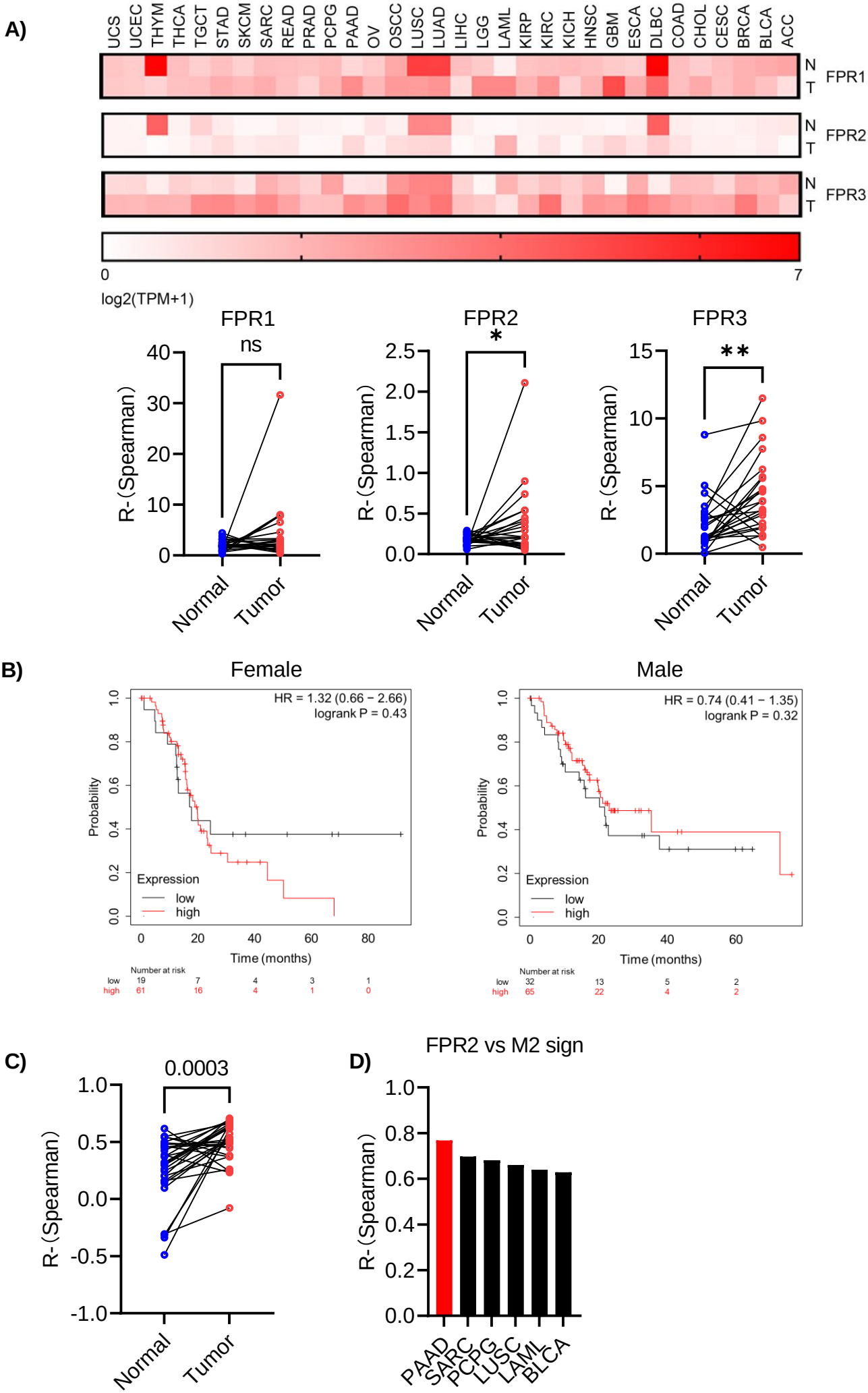

Supplementary Figure 1. FPRs correlate with pro-cancer macrophage signatures **A)** Heatmap visualization and paired comparison of the gene expression levels of FPR1, FPR2, and FPR3 in different cancer tissues (T) and the matched normal tissues (N) in the TCGA datasets. Data are shown as log2 (TPM+1). **B)** Kaplan–Meier survival curves comparing FPR3 low and high mRNA expression levels total PAAD cohort, in female, and male patients, respectively. Survival curves based on overall survival (OS) are shown. **C)** Overall comparison of Spearman's rank correlation coefficients for FPR2 with M2 macrophage signature for a total of 30 types of tumors and normal tissues from TCGA datasets. Wilcoxon tests were performed. **D)** Results of Spearman's rank correlation analyses of FPR2 with M2 macrophage signature genes using TCGA datasets plotted with coefficient R and -log10 (P-value). The six most significant tumor types are shown.

He et. al. Supplementary Figure 2.

A)

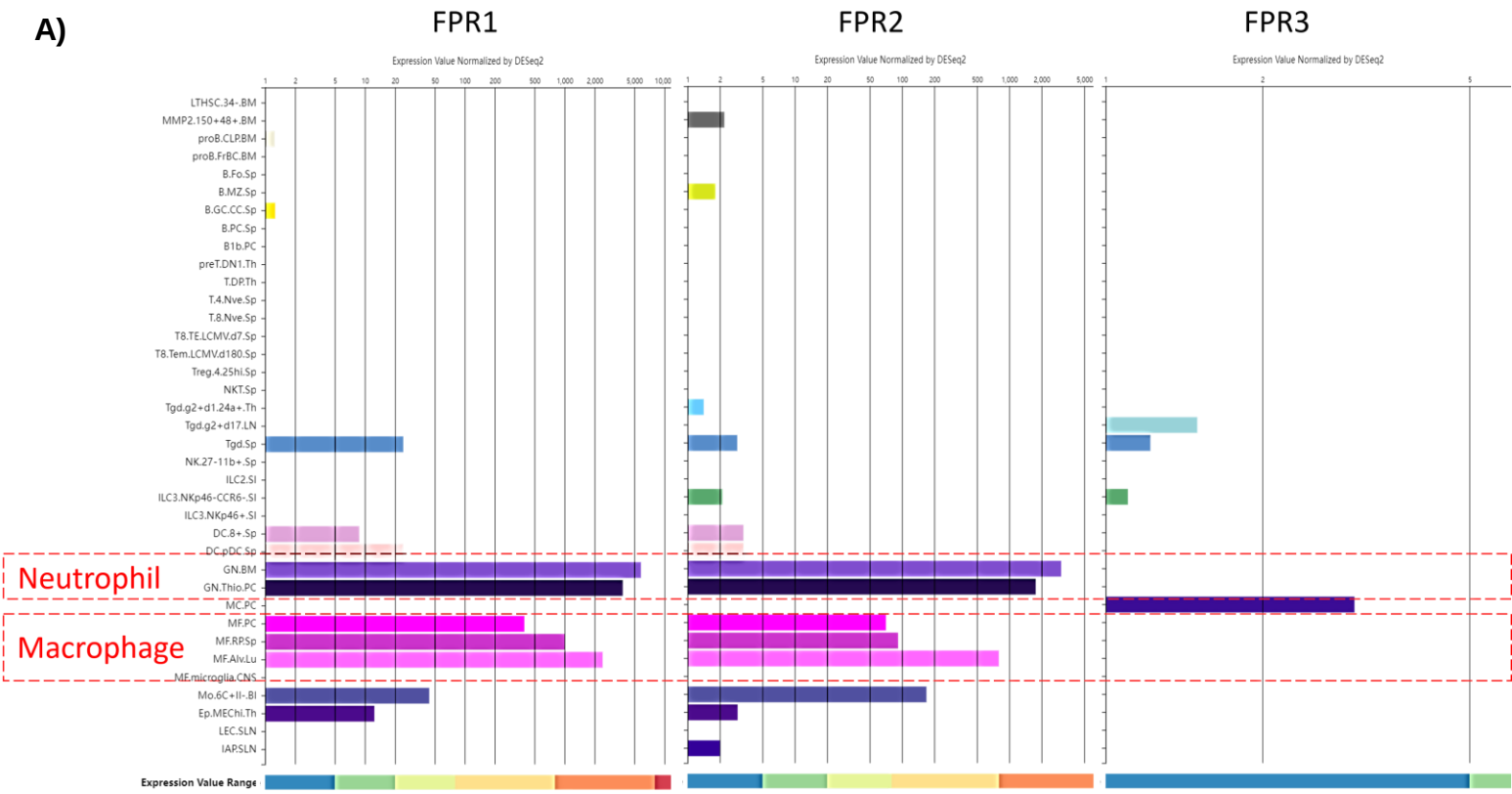

B)

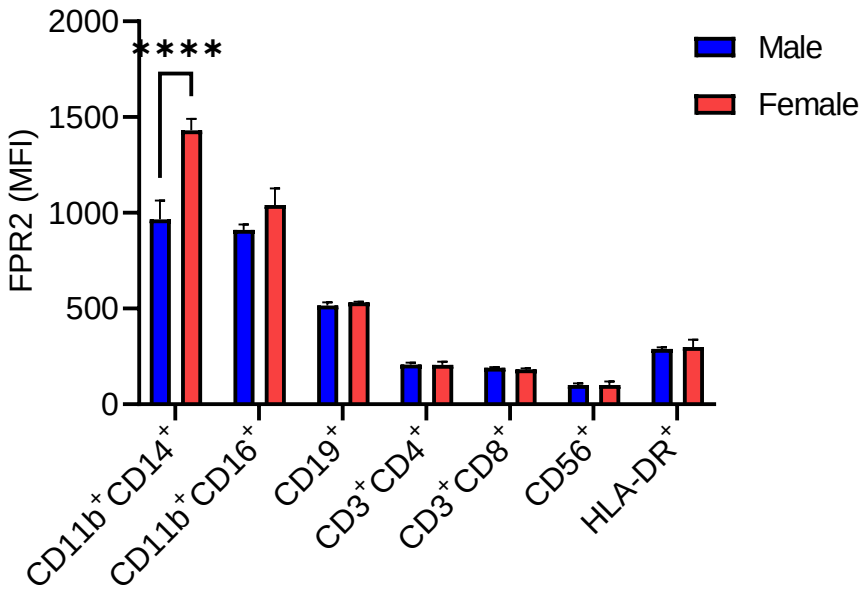

Supplementary Figure 2. Human gene and protein expression in different immune cell types

A) FPR1 (205118_at), FPR2 (210773_at), and FPR3 (214560_at) mRNA expression levels in Primary Cell Atlas in BioGPS Dataset website. Data is publicly available from BioGPS portal. **B)** FPR2 expression (MFI) in human peripheral blood mononuclear cells analyzed by flow cytometry (n=2). Data is shown as mean±SEM.

He et. al. Supplementary Figure 3.

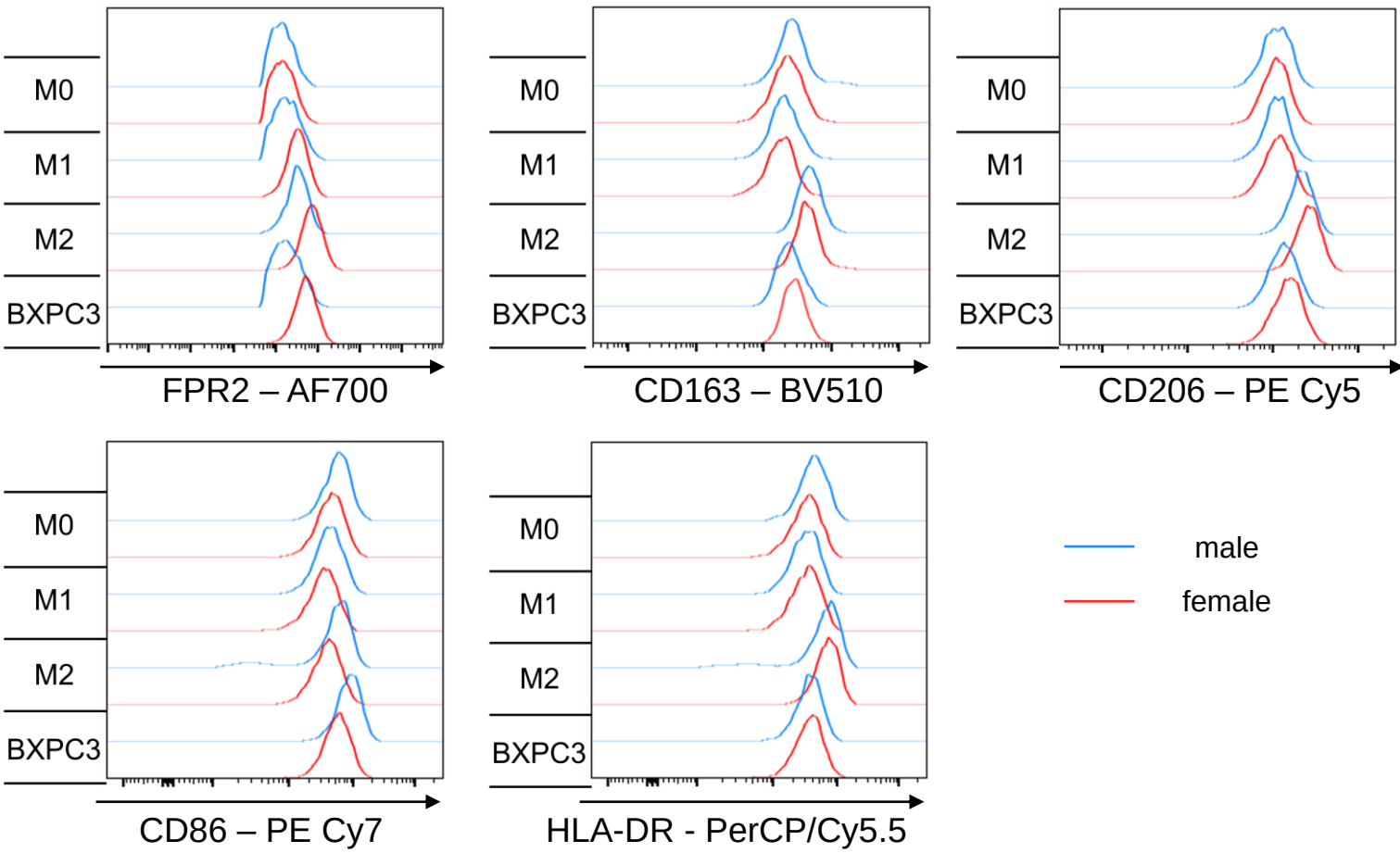

Supplementary Figure 3. FPR2 is differentially expressed in macrophages of different sexes

Representative flow cytometry histogram of FPR2 and classical macrophage markers are shown. M0, M1, M2 and tumor conditional macrophages (BxPC3) were compared sequentially, male vs. female.

He et. al. Supplementary Figure 4.

A)

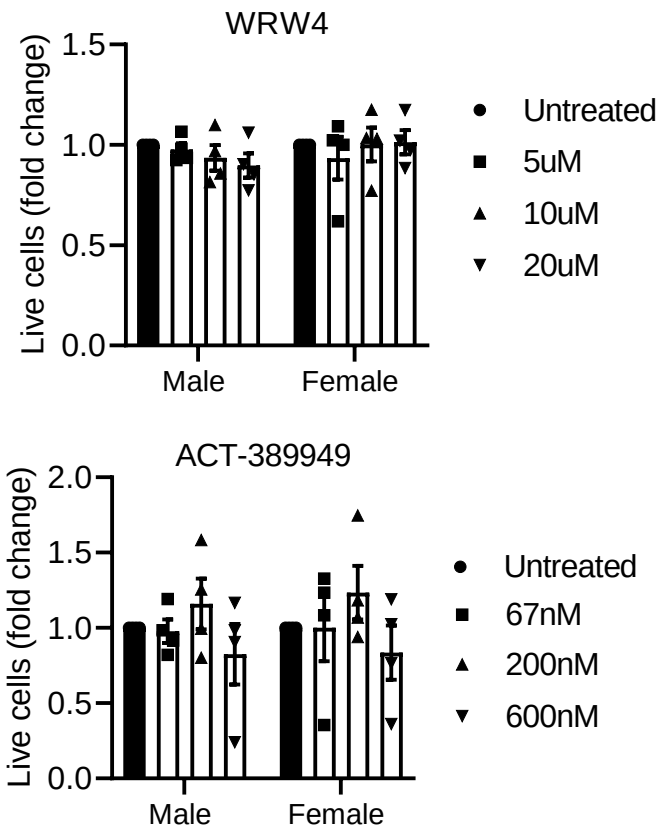

B)

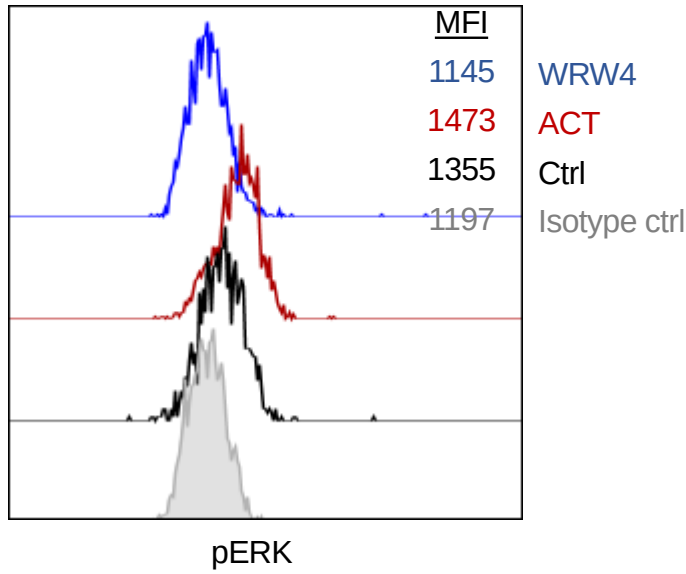

C)

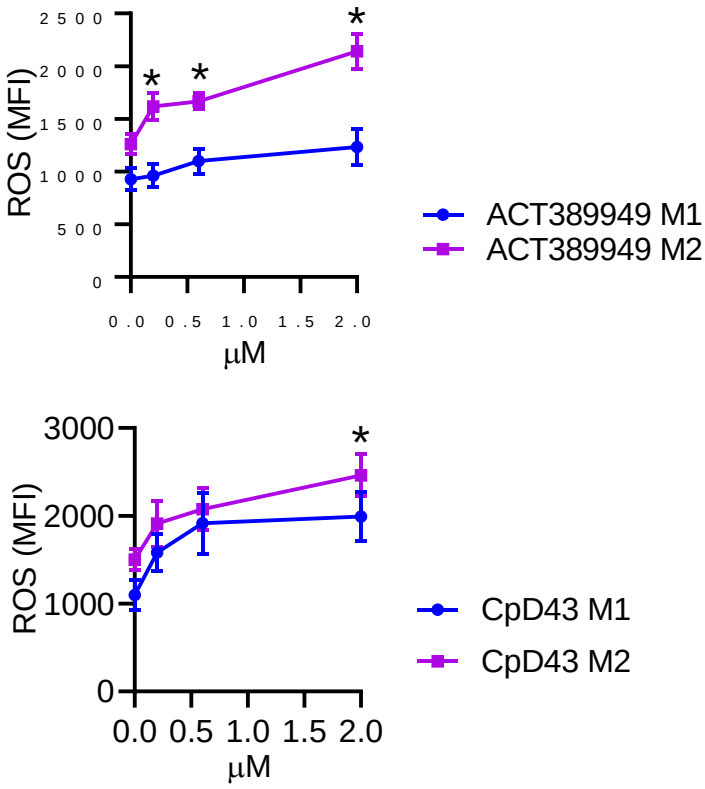

Supplementary Figure 4. Pharmacological targeting of FPR2

A) Percentage of live cells after 72-hour incubation of induced macrophages with 0-600 nM FPR2 agonist (ACT-389949) or 0-20μM antagonist (WRW4) and assessed for viability. **B)** A representative histogram (n=4) of pERK expression in M2 macrophages cultured with the indicated treatments. **C)** ROS production in macrophages treated with FPR2 agonists (ACT-389949 or CpD43). M1 and M2 macrophages were induced from the same HD-derived macrophages, and treated with different concentration gradients of FPR2 agonists, respectively. (n=4 HD/group; *$p < 0.05$)

He et. al. Extended Data Figure 5.

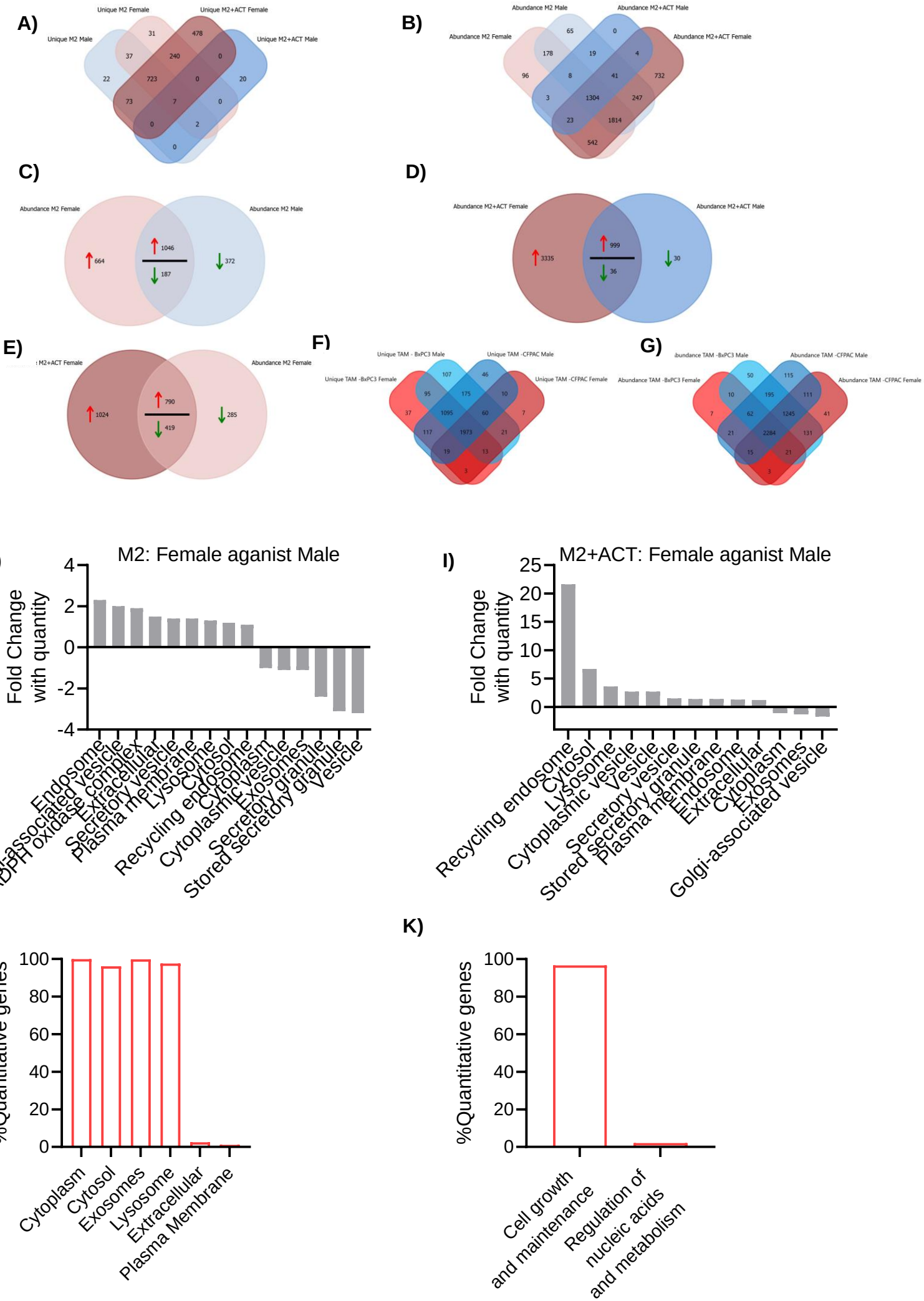

Supplementary Figure 5. Proteomics of macrophages targeted by FPR2 agonist ACT-389949

A-B) Venn Diagram of the unique proteins identified and their corresponding protein abundances in M2 with and without ACT treatment. **C-E)** Fold change comparison of proteins with abundances between males and females and within the same sex. Fold change of 2 and above was used for comparison. **F-G)** Unique proteins identified and their corresponding protein abundances in TCM (BxCP3 and CFPAC). **H-J)** FunRich quantitative gene ontology in cellular compartment comparing females to males with or without ACT treatment, alternatively, TCM. **K)** Quantitative gene ontology analysis of biological processes, **L)** biological pathways, and **M)** transcription factors. Accumulative data of all proteins are shown (n=4 biological replicates each condition and sex) with FDR≤0.01 confidence, are master proteins and present in two out of three technical replicates.

He et. al. Supplementary Figure 6.

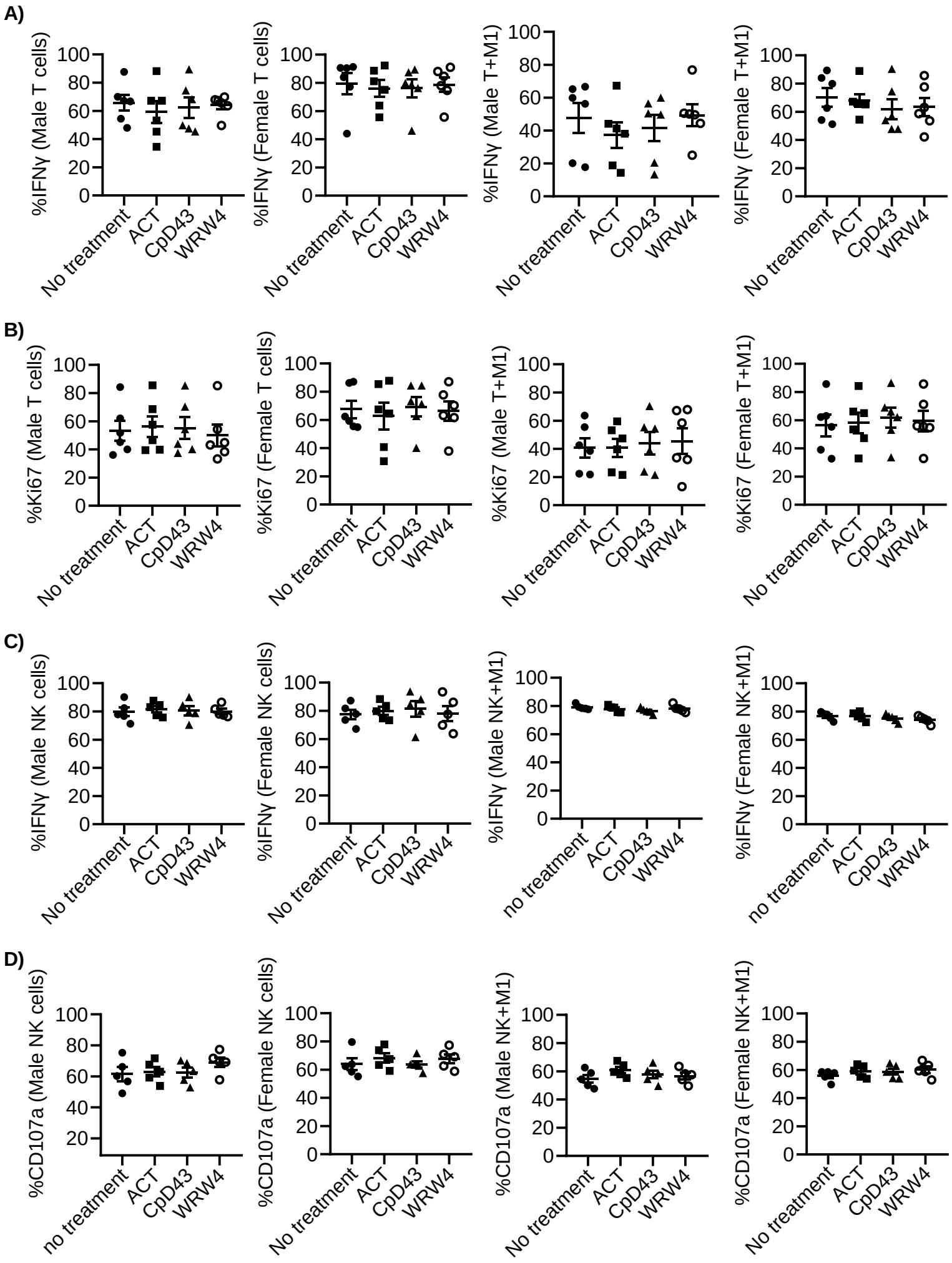

Supplementary Figure 6. FPR2 agonist and antagonist had no effect on M1-type macrophages and effector cells cultured alone

A) Quantification of %IFN-γ^+ T cells. **B)** Quantification of %Ki67$^+$ T cells. **C)** Quantification of %IFN-γ^+ NK cells. **D)** Quantification of %CD107a$^+$ NK cells. The four groups male effector cell alone, female effector cell alone, male effector cell with M1, female effector cell with M1 are shown sequentially from left to right as mean±SEM.

He et. al. Supplementary Figure 7.

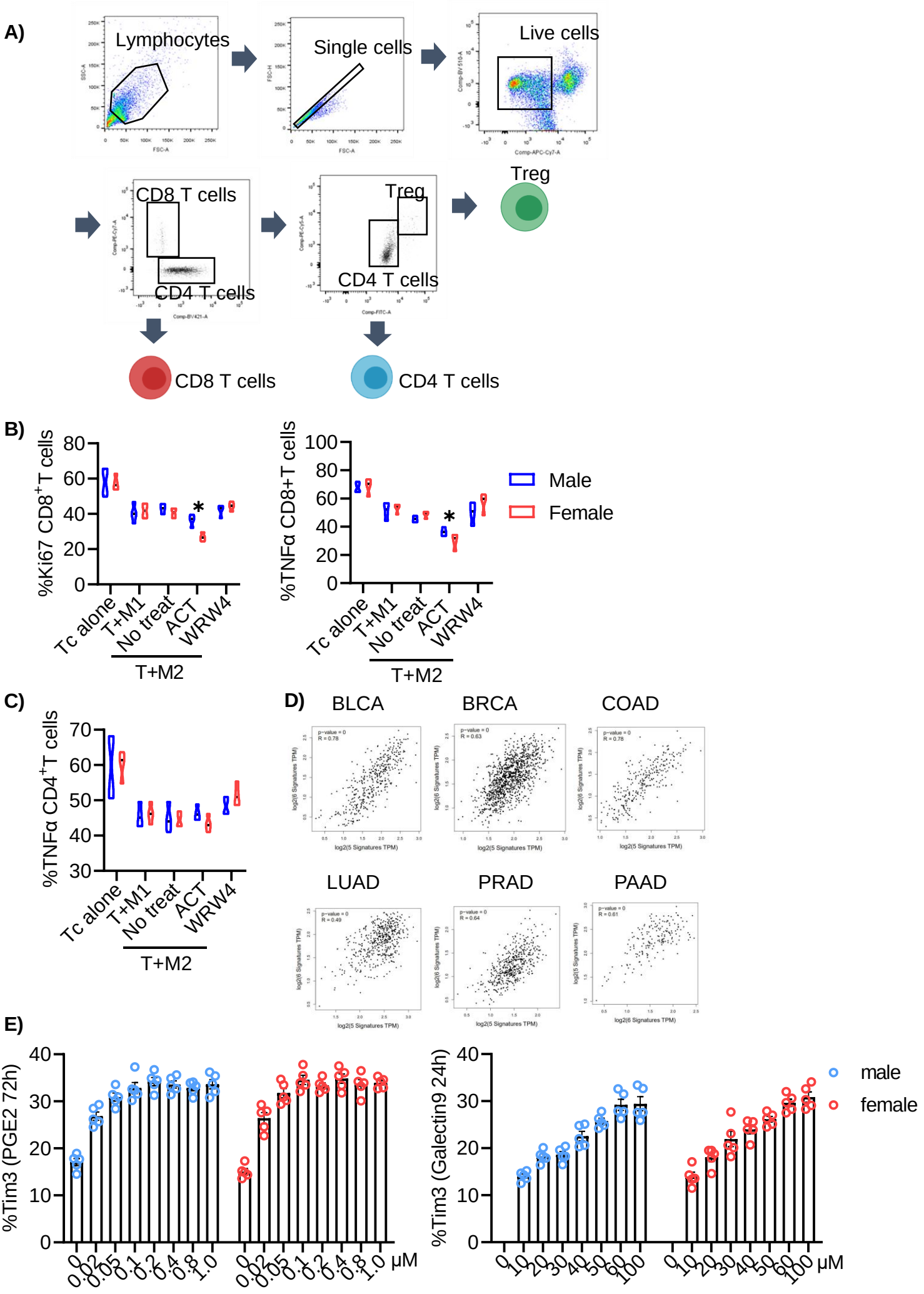

Supplementary Figure 7. Specific activation of FPR2 in macrophages enhances immunosuppression of T cells

A) Gating strategy for flow cytometry analysis. Purified T cells were gated on size, single cells, and live cells and thereafter for positive expression of CD3/CD4/CD8/CD25/FoxP3. **B)** Quantification of percent $Ki67^+$ and $TNF\alpha^+$ CD8 T cells is shown (n=4) and **C)** $\%TNF\alpha^+$ CD4 T cells. **D)** Correlations of M2 macrophage signature and T-cell exhaustion signature from six tumor types extracted from the TCGA datasets. **E)** Quantification of $Tim3^+$ T cells (n=5) following stimulation by recombinant PGE2 and Galectin9. Data shown as mean±SEM.

He et. al. Supplementary Figure 8.

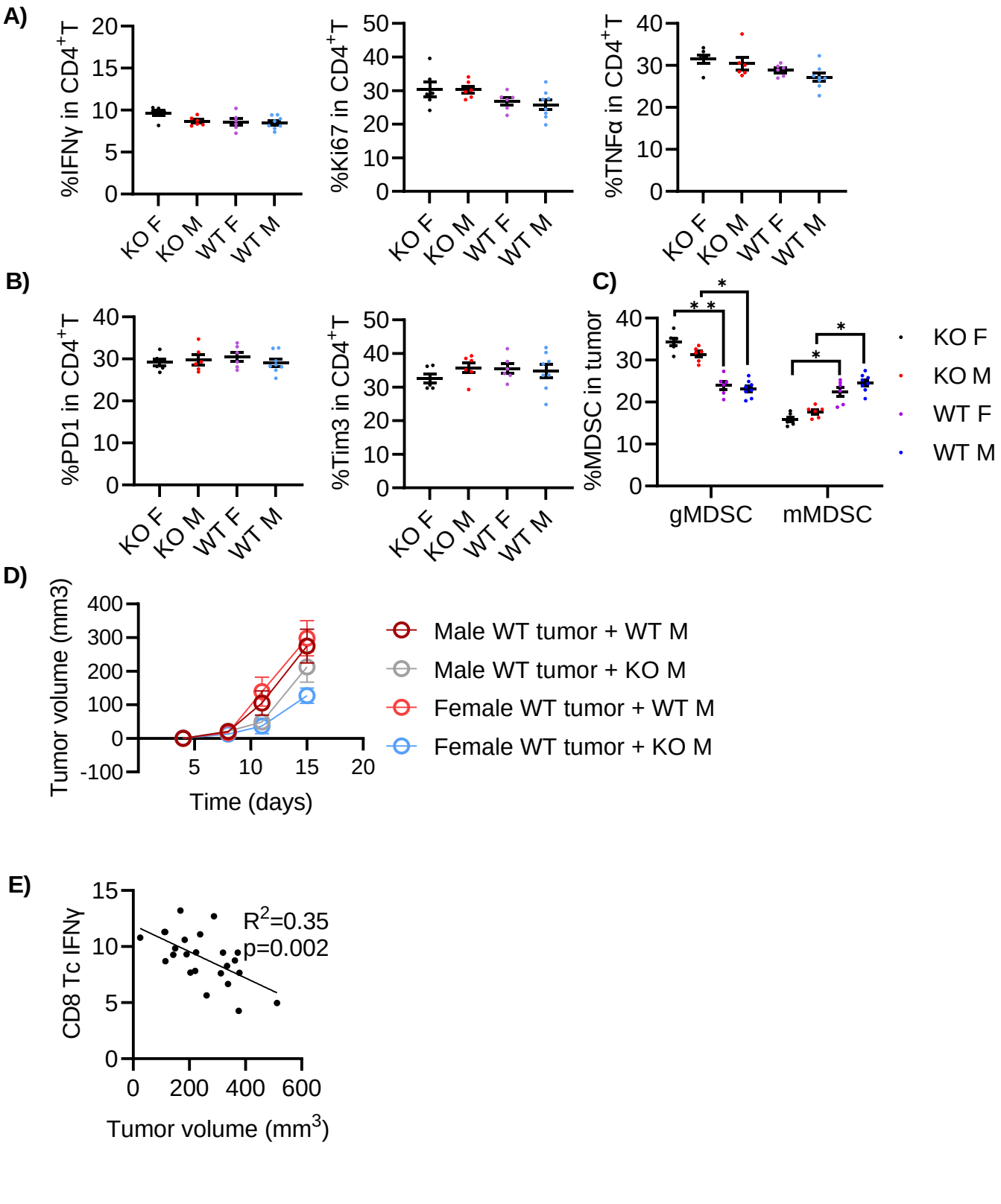

Supplementary Figure 8. FPR2 regulates myeloid function and suppresses anti-tumor T cell response in the tumor microenvironment *in vivo*

A) % IFNγ, %Ki67 and, %TNFα, detected in KPC tumor-infiltrating $CD4^+$ T cells. **B)** % PD1 and %Tim3 detected in KPC tumor-infiltrating $CD4^+$ T cells. **C)** %gMDSC and %mMDSC in KPC tumor-infiltrating leukocytes.**D)** Tumor growth curves of KPC subcutaneous tumor model with macrophage transferred and **E)** Intratumoral CD8 T cell IFNγ production correlation with the tumor growth.

Table 1. Antibodies and dyes used in the study

Human Antibodies			
Epitope	Color	Clone	Company
FPR2	Primary	GM1D6	Invitrogen
Pan-ck	Primary	AE1/AE3 + 5D3	abcam
CD3	Primary	SP7	abcam
CD45	AF488	H130	Biolegend
CD11b	APC	ICRF44	Biolegend
Dead cell marker	Near-IR		Thermofisher
CD14	APC/Cy7	63D3	Biolegend
FPRL1/FPR2	AF700	304405	RD systems
CD163	BV510	GHI/61	BD Biosciences
CD206	PE Cy5	551136	BD Biosciences
CD86	PE Cy7	SK1	Biolegend
HLA-DR	PerCP/Cy5.5	Tü36	Biolegend
CD3	BV510	HIT3a	BD Biosciences
CD4	BV421	RPA-T4	BD Biosciences
CD8	PE-CY7	SK1	Biolegend
CD56	PE Cy7	BC96	Biolegend
CD56	APC	5.1H11	Biolegend
IFNγ	BV650	4S.B3	Biolegend
Ki67	AF700	B56	BD Biosciences
CD107a	PerCP/Cy5.5	H4A3	Biolegend
PD1	APC	eBioJ105	Invitrogen
Tim3	BV605	F38-2E2	Biolegend
TNFα	BV786	MAB11	Biolegend
CD16	PE	3G8	Biolegend
CD19	PECy5	1D11	BioSite
FoxP3	AF488	PCH101	Invitrogen
CD25	PE/Cy5	BC96	Biolegend
Fc Block			BD Biosciences
Human Block Antibodies			
Purified anti-human CD366 (TIM3)			Biolegend
Purified anti-human CD279 (PD-1)			Thermofisher
Murine Antibodies			
FPR2	Primary	Polyclonal	abcam
F4/80	PECy5	CI:A3-1	Biolegend
CD206	AF488	C068C2	Biolegend
LY6C	PE-Cy7	AL-21	BD Biosciences
LY6G	BV711	1A8	BD Biosciences
CD11b	BV605	M1/70	BD Biosciences
CD3	BV421	17A2	Biolegend
CD4	BV785	RM4-5	BD Biosciences

CD8a	BV421	53-6.7	BD Biosciences
IFNγ	PerCP/Cy5.5	XMG1.2	BD Biosciences
TNFα	PE	MP6-XT22	BD Biosciences
Ki67	AF700	B56	BD Biosciences
PD1	BV510	J43	BD Biosciences
Tim3	APC	5D12	BD Biosciences
CD25	BV650	PC61	BD Biosciences
CD45	AF647	16A	BD Biosciences

Table 2. Primers used in the study

Gene name	Oligo name	Tm°C	Sequence 5'-3'
IL1RN	F	58.9	CTCAGCCAACACTCCTAT
	R	60	TCCTGGTCTGCAGGTAA
IL2	F	63.8	AGAACTCAAACCTCTGGAGGAAG
	R	64.7	GCTGTCTCATCAGCATATTCACAC
IL4	F	68.6	CCGTAACAGACATCTTTGCTGCC
	R	66.7	GAGTGTCCTTCTCATGGTGGCT
IL10	F	65.9	ACATCAAGGCGCATGTGAACT
	R	65.5	TGGCTTTGTAGATGCCTTTCTCTT
CD274	F	67.0	TGCCGACTACAAGCGAATTACTG
	R	68.1	CTGCTTGTCCAGATGACTTCGG
LGALS9	F	68.8	TGCAACACGAGGCAGAACG
	R	66.4	CACAGAGCCATTGACGGAGAT
IL12p40	F	62.3	CCAAGAACTTGCAGCTGAAG
	R	62.5	TGGGTCTATTCCGTTGTGTC
TGFB	F	67.4	TACCTGAACCCGTGTTGCTCTC
	R	69.3	GTTGCTGAGGTATCGCCAGGAA
PTGS2	F	59.6	TTCAAATGAGATTGTGGGAAAT
	R	63.7	AGATCATCTCTGCCTGAGTATCTT
GAPDH	F	65.1	ACCATCATCCCTGCCTCTAC
	R	62.3	CCTGTTGCTGTAGCCAAAT